Block Copolymer Adsorption from a Homopolymer Melt to Silicon Oxide: Effects of Nonadsorbing Block Length and Anchoring Block−Substrate Interaction

Ana Claudia Costa,[†] Mark Geoghegan,[‡] Petr Vlček,[§] and Russell J. Composto*,[†]

Department of Materials Science and Engineering, Laboratory for Research on the Structure of Matter, University of Pennsylvania, Philadelphia, Pennsylvania 19104; Department of Physics and Astronomy, University of Sheffield, Hounsfield Road, Sheffield S3 7RH, United Kingdom; and Institute of Macromolecular Chemistry, Academy of Sciences of the Czech Republic, Prague, Czech Republic

Received June 18, 2003; Revised Manuscript Received August 28, 2003

ABSTRACT: The adsorption of block copolymers from a homopolymer matrix is studied as a function of nonadsorbing block length and adsorbing block type. The copolymers are poly(deuterated styrene-*block*-methyl methacrylate), dPS-*b*-PMMA, and poly(deuterated styrene-*block*-(dimethylamino)ethyl methacrylate), dPS-*b*-PDMAEMA, where the PMMA and PDMAEMA blocks adsorb to silicon oxide, SiO_x, and the dPS block extends into a polystyrene, PS, matrix. Using neutron reflectivity and low-energy forward recoil spectrometry, the volume fraction profile, $\phi(z)$, copolymer interfacial excess, z^*, interfacial width, w, and adsorbed layer thickness, h, are investigated as a function of the degree of polymerization of the dPS block, N_{dPS}. For $N_{dPS} < 200$, the distance between grafted copolymer chains, D, is greater than the dPS radius of gyration, R_g, whereas for $N_{dPS} > 200$, D is less than R_g. Thus, a crossover from a collapsed to a stretched conformation occurs near the N_{dPS} for entanglements in PS. Correspondingly, z^*, w, and h strongly increase as N_{dPS} increases. Using an adsorbing block−substrate interaction parameter that depends on the adsorbing block length, self-consistent mean-field predictions of $\phi(z)$, z^*, w, and h are in very good agreement with experimental results. By considering the fraction of adsorbing block segments in direct contact with the wall, the segmental interaction energies between MMA and SiO_x and DMAEMA and SiO_x are about $-0.8\ k_BT$ and $-1.1\ k_BT$, respectively, consistent with a stronger affinity of DMAEMA to the oxide.

1. Introduction

The properties of adhesives, coatings, colloidal stabilizers, and paints strongly depend on the affinity between polymers and inorganic substrates as well as the conformation of these adsorbed polymers. Although interfacial properties are determined by these two factors, the interaction strength between a polymer and a substrate cannot be easily determined experimentally and is not readily available in the literature. In fact, few experimental studies attempt to measure the strength of these interactions.[1−9] However, the polymer conformation near interfaces has been studied theoretically[2,9−11] and experimentally.[12−16] The goals of our study are to investigate the effects of the nonadsorbing block length on the conformation of adsorbed molecules at the polymer/substrate interface and to understand how these interfacial characteristics depend on the polymer−substrate interaction by changing the adsorbing block type.

In general, the interactions between a polymer chain and substrate are due to van der Waals or other secondary bonds. Furthermore, the strength and type of interactions with the substrate, which determine the conformation of the adsorbed polymer molecules at the interface, are influenced by the degree of polymerization, DP, the Flory−Huggins segment−segment interaction parameter, χ, and the affinity between each segment and the substrate. Thus, in addition to anchor strength, the degree of interpenetration between the free ends of the adsorbed chains and the matrix chains can promote adhesion. For the case of an adsorbed block copolymer in a homopolymer matrix, the interfacial width and chain conformation near the interface are mainly governed by the DPs of the matrix, P, and the nonadsorbing block, N_{dPS}, as well as the strength of the interaction between the adsorbing block and the substrate.

For a poly(deuterated styrene-*block*-methyl methacrylate), dPS-*b*-PMMA, block copolymer adsorbed to silicon oxide, SiO_x, from a polystyrene, PS, matrix, the dPS interfacial excess, z^*, has been shown to initially increase rapidly with P and then become constant for $P > 2N_{dPS}$.[2] Oslanec et al.[2] have attributed this behavior to the increasing entropic repulsion of matrix chains from the adsorbed block copolymer. Thus, as P increases, the molecules cross over from a stretched to a collapsed conformation. Using low-energy forward recoil spectrometry, LE-FRES, and neutron reflectivity, NR, Oslanec et al.[9] have also studied block copolymer adsorption as a function of matrix species. For dPS-*b*-PMMA adsorbed at the film/SiO_x interface from a poly(styrene-*ran*-4-bromostyrene), PBr_yS, matrix, z^* was found to decrease as the bromostyrene mole fraction, y, was systematically increased. Assuming that the PBr_yS chains did not interact with the substrate, self-consistent mean-field, SCMF, calculations predicted that z^* increased as y increased because of the unfavorable PBr_yS−dPS interaction. Upon including a small attraction between PBr_yS chains and SiO_x, z^* decreased as y increased in agreement with experiment. Thus, SCMF results showed that PBr_yS competed with dPS-*b*-PMMA for SiO_x and effectively canceled the expected increase

[†] University of Pennsylvania.
[‡] University of Sheffield.
[§] Academy of Sciences of the Czech Republic.

10.1021/ma0348324 CCC: $25.00
Published on Web 11/26/2003

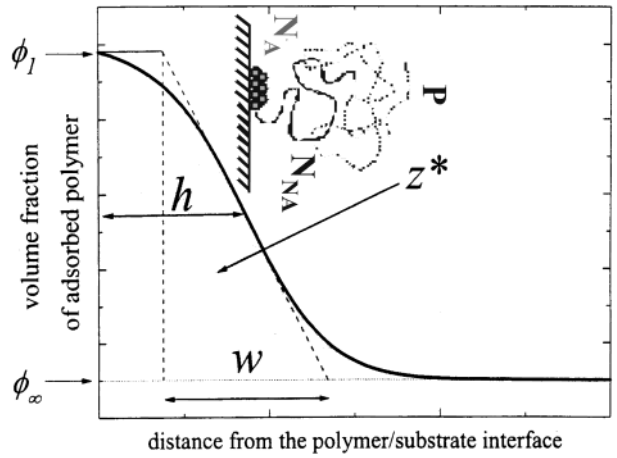

Figure 1. Schematic of the volume fraction profile of an adsorbed layer. The interfacial characteristics are defined: interfacial width, w, adsorbed layer thickness, h, and interfacial excess, z^*. The surface and bulk volume fractions are ϕ_1 and ϕ_∞, respectively. The system parameters are noted in the inset, where N_A, N_{NA}, and P represent the DP of adsorbing block, nonadsorbing block, and matrix, respectively.

in dPS-*b*-PMMA adsorption due to the unfavorable interaction between dPS and PBr$_y$S. In the present paper, the interaction strength between the adsorbing block of the copolymer and the substrate is varied directly by changing the anchoring block type rather than the matrix species.

Using NR, Retsos et al.[10] studied the adsorption of diblock copolymers as a function of the ratio of adsorbing to nonadsorbing block lengths. By varying the ratios of block lengths, the nonadsorbing block was found to form either a "wet brushlike" or a "mushroomlike" conformation with a transition occurring over a wide range of block lengths. In these studies, the nonadsorbing block length was fixed and the anchoring block varied. In the present system, the adsorbing block length is kept nearly constant whereas the nonadsorbing block length varies by 1 order of magnitude from $N_{dPS} = 94$ to 933. This range is particularly interesting because the dPS block varies from shorter to longer than the entanglement DP of PS, N_e, = 194.[17]

Figure 1 represents a volume fraction profile of an adsorbed layer, $\phi(z)$. From this profile, one can determine the interfacial excess, z^*, the thickness of the adsorbed layer, h, and the interfacial width between the adsorbed layer and the bulk, w. In Figure 1, the interfacial excess, z^*, is defined as the area under $\phi(z)$ in excess of the bulk volume fraction, ϕ_∞. Thus, z^* is described by

$$z^* = \int_0^\infty dz\ (\phi(z) - \phi_\infty) \tag{1}$$

Knowing z^*, the graft density of chains can be determined:

$$\sigma = z^* \rho N_{av}/(N_{dPS} M_0) \tag{2}$$

where ρ is the polymer density, N_{av} is Avogadro's number, and M_0 is the relative molar mass of a PS monomer. The thickness of the adsorbed layer is defined by

$$h = (1/z^*)\int_0^\infty z(\phi(z) - \phi_\infty)\, dz \tag{3}$$

Table 1. Characteristics of dPS-*b*-PMMA Block Copolymers

M_w (g/mol)	$M_{w,dPS}$ (g/mol)	N_{dPS}	N_{PMMA}	PDI
11 000	9 800	94	10	1.21
22 500	17 600	169	48	1.20
50 000	46 280	445	37	1.21
110 000	104 700	933	44	1.05

Table 2. Characteristics of dPS-*b*-PDMAEMA Block Copolymers

M_w (g/mol)	$M_{w,dPS}$ (g/mol)	N_{dPS}	$N_{PDMAEMA}$	PDI
43 000	39 990	356	19	1.20
76 500	75 720	676	6	1.11

The interfacial width, w, is determined by the slope of the profile at the inflection point as shown in Figure 1. A steep slope indicates a narrow interface with little interpenetration between the adsorbed layer and the free matrix and copolymer chains. On the other hand, a broad interface suggests a high degree of interdigitation between adsorbed and free chains.

The interfacial characteristics represented in Figure 1 are governed by the molecular parameters of the system. As shown in the inset of Figure 1, these parameters include the DPs of the matrix, P, the nonadsorbing block, N_B, and the anchoring block, N_A. Moreover, segment−segment interaction parameters and the interaction energies between segments and the substrate are important. In this paper, the adsorbed copolymer is found to vary from a collapsed to a stretched conformation as N_{dPS} increases from 94 to 933. The experimental volume fraction profiles are in very good agreement with those from a SCMF model containing only one fitting parameter, namely the interaction strength between each copolymer block and the substrate, Σ. By including the fraction of anchoring monomers in contact with the substrate, a constant segment interaction energy, ϵ, is observed.

2. Experimental Section

2.1. Materials and Sample Preparation. Two types of asymmetric block copolymers were synthesized using anionic polymerization. The first is poly(deuterated styrene-*block*-methyl methacrylate), dPS-*b*-PMMA, with the four molar masses listed in Table 1. The three highest molar mass copolymers have a nearly constant DP for the adsorbing PMMA block ($N_{PMMA} \approx 40$) and a varying dPS dangling block length, N_{dPS}, which extends away from the substrate. To investigate the role of entanglements, N_{dPS} was varied from 94 to 933. For comparison, N_e of PS is 194.[17] The second block copolymer is poly(deuterated styrene-*block*-(dimethylamino)-ethyl methacrylate), dPS-*b*-PDMAEMA, having the two molar masses listed in Table 2. Note that both N_{dPS} and $N_{PDMAEMA}$ were varied. Tables 1 and 2 also include the copolymer molar masses and polydispersity indexes, PDI, which were both determined by size exclusion chromatography. The chemical composition (N_{PMMA} and $N_{PDMAEMA}$) was characterized by ^{13}C nuclear magnetic resonance.

Because the interaction of the dPS block with SiO_x is relatively weak,[2,9] the PMMA and PDMAEMA blocks are responsible for anchoring each copolymer to the substrate.[4,18] These copolymers were blended into a matrix of PS with a degree of polymerization, P, and PDI of 1923 and ≤1.06, respectively. The PS was purchased from Pressure Chemical. The PS matrix represents a nearly neutral environment for the dPS blocks of both copolymers. To ensure that the interfacial characteristics are independent of P, all blends obeyed the condition $P > 2N_{dPS}$.[2]

Silicon oxide surfaces were prepared by first etching as-received silicon wafers for 3 min in a hydrofluoric acid:water

solution (1:7) to remove the native oxide. Then wafers were placed in an ultraviolet ozone cleaner for 10 min to grow a clean SiO_x layer. The SiO_x characteristics were given previously.[19] The polymer films were prepared by spin-coating a solution of 3.0 wt % polymer in toluene at 2000 rpm for 60 s on a fresh SiO_x surface. The solutions were filtered prior to spin-casting to remove dust particles. The polymer concentrations were 5 vol % diblock copolymer (dPS-*b*-PMMA or dPS-*b*-PDMAEMA) and 95 vol % PS. The polymer films were dried in a vacuum oven at 110 °C (above the glass transition temperature of PS) for 12 h to ensure complete solvent removal. The film thickness values measured by ellipsometry ranged from 178 to 183 nm. After drying and prior to analysis, samples were annealed in a vacuum oven at 175 °C for 5 days. This annealing time was long enough to ensure equilibrium adsorption.[2] For selected studies, LE-FRES experiments were also performed on samples containing only bound copolymer. Annealed samples were immersed in toluene for approximately 48 h to remove free matrix and block copolymer chains and then dried overnight in a vacuum oven at 110 °C. Relative to the blend films, the LE-FRES spectrum of the copolymer alone had a greatly improved signal-to-noise ratio which was particularly important for determining the low z^* values for short copolymers, i.e., $N_{dPS} < N_e$.

2.2. Neutron Reflectivity and Low-Energy Forward Recoil Spectrometry. LE-FRES and NR experiments were performed to determine the interfacial characteristics of the adsorbed layer. From in-house LE-FRES experiments, z^* of the dPS block was measured using a 2.0 MeV He^+ ion beam at 15° incident and exit angles with respect to the polymer film and a 6 μm Mylar stopper filter. Under these conditions, LE-FRES has a depth resolution of 50 nm at the surface and 60 nm at 180 nm beneath the surface. Interfacial excess values as low as 0.5 nm can be measured under these conditions. Conventional LE-FRES has been described elsewhere.[20] Because of its superior depth resolution, ≈0.3 nm, NR can be used to determine the volume fraction profile of the adsorbed copolymer as well as the interfacial characteristics (h, w, and σ).

The NR experiments were performed at the National Cold Neutron Research (NCNR) facility at the National Institute of Standards and Technology (NIST) on the NG7 Reflectometer. The principles of NR have been described elsewhere.[21] Because reflectivity is obtained in reciprocal (momentum) space, different depth profiles can sometimes be used to predict reflectivities in good agreement with the measured reflectivity. For this reason LE-FRES is particularly useful because it can eliminate complications such as surface segregation and provide input parameters for NR fitting. The NR data were evaluated using an error function to capture the interfacial profile of the copolymer adsorbed to SiO_x. The error function profile has two variable parameters, an offset and a width, which can be used to simulate either an exponential decay or a parabolic profile. The reflectivity was calculated using a recursive routine. The profile was divided into 50 layers having different thicknesses but the same change in neutron scattering length density (i.e., volume fraction) between adjacent layers.[6] The fits were minimized using a downhill simplex fitting routine.[22]

3. Self-Consistent Mean-Field Model

A SCMF model was used to simulate the block copolymer volume fraction profile at the polymer/solid interface. The SCMF model followed the approach developed by Shull and Kramer.[23,24] In brief, the model assumed a segment density profile to determine a mean field, which was then used to solve a diffusion equation that recalculated a new segment profile. The lattice size is based on the styrene monomer, 0.67 nm. The input parameters for the SCMF model reflect the materials characteristics, blend thermodynamics, and block−substrate interaction parameters. For the PS:dPS-*b*-PMMA system the input parameters that were held constant include N_{PMMA}, N_{dPS}, P, $\chi_{PMMA-dPS}$, $\chi_{PMMA-PS}$, and χ_{dPS-PS}. For the PS:dPS-*b*-DMAEMA system, the fixed input parameters were $N_{PDMAEMA}$, N_{dPS}, P, $\chi_{PDMAEMA-dPS}$, $\chi_{PDMAEMA-PS}$, and χ_{dPS-PS}. The only parameter that was allowed to vary was the interaction energy between the adsorbing block and substrate, $\Sigma_{PMMA-SiO_x}$ (or $\Sigma_{PDMAEMA-SiO_x}$). From Σ, the segment interaction energy, ϵ, can be determined. The interaction energies between the nonadsorbing block and substrate as well as the matrix and substrate were taken as 0. In the simulations, the dPS block and PS interactions with the SiO_x substrate were too weak to have a measurable effect on interfacial properties. For example, the interfacial properties changed by 5% at most if a small attractive interaction of $-0.01k_BT$ between PS and dPS segments with SiO_x substrate was assumed. Note that this value is 1 order of magnitude weaker than the ϵ between PMMA and SiO_x. This observation is consistent with those of Oslanec et al.[2,8] Therefore, only one input parameter $\Sigma_{PMMA-SiO_x}$ (or $\Sigma_{PDMAEMA-SiO_x}$) was systematically varied until the SCMF profile fell into good agreement with the experimental profile (cf. Figures 8 and 9).

4. Results and Discussion

4.1. Interfacial Characteristics of PS:dPS-*b*-PMMA Films. For the PS:dPS-*b*-PMMA system, the vol % of dPS-*b*-PMMA in the blend is 5. The PS matrix had a $P = 1923$ ($>2N_{dPS}$). Parts a and b of Figure 2 show the experimental reflectivity, R (solid circles), vs wavevector, k, for the dPS-*b*-PMMA with the shortest, 94, and the longest, 933, blocks of dPS, respectively. The oscillations are mainly due to constructive interference of neutrons from the top and bottom of the film surfaces. The calculated R values (solid lines) are determined from the volume fraction profiles shown in Figure 2c (for $N_{dPS} = 94$) and Figure 2d (for $N_{dPS} = 933$). As previously discussed, the profiles were fitted to error functions, which, depending upon the offset and width of the function, can be simulated to exponential decays or parabolic profiles. For the shortest block (cf. Figure 2c) the profile shape is exponential-like and described by the function $\phi(z) = 0.04 + 0.75 \exp[(-z/2.55)$. However, for the longest block (cf. Figure 2d) the shape is parabolic-like and given by $\phi(z) = 0.57787(1 - 0.00002z^2)$. In both profiles, the vol % of dPS-*b*-PMMA in the bulk is 4 accounting for the conservation of mass, and z has units of nanometers. Based on the profiles for all four copolymers, the optimum profile shape is more exponential-like for $N_{dPS} < N_e$ and parabolic-like for $N_{dPS} > N_e$. Thus, as N_{dPS} increases, the dPS block extends further into the matrix, resulting in a broader interfacial width. The dPS$-SiO_x$ interface is at depth 0. Note that the depletion of dPS near the oxide for $N_{dPS} = 933$ (cf. Figure 2d) suggests that the PMMA anchor layer becomes thicker (i.e., more loops) and makes fewer contacts with the oxide. This issue will resurface when the SCMF results are interpreted. Finally using eq 1, z^* can be calculated and is found to increase from 1.9 to 5.9 nm as N_{dPS} increases from 94 to 933, respectively.

Figure 3 shows that z^* increases by nearly a factor of 6 as N_{dPS} increases by ∼10×. For each value of N_{dPS}, z^* is determined by NR and LE-FRES on films and LE-FRES from the physisorbed copolymer layer alone after removing free chains with toluene. The LE-FRES measurements are in good agreement, demonstrating

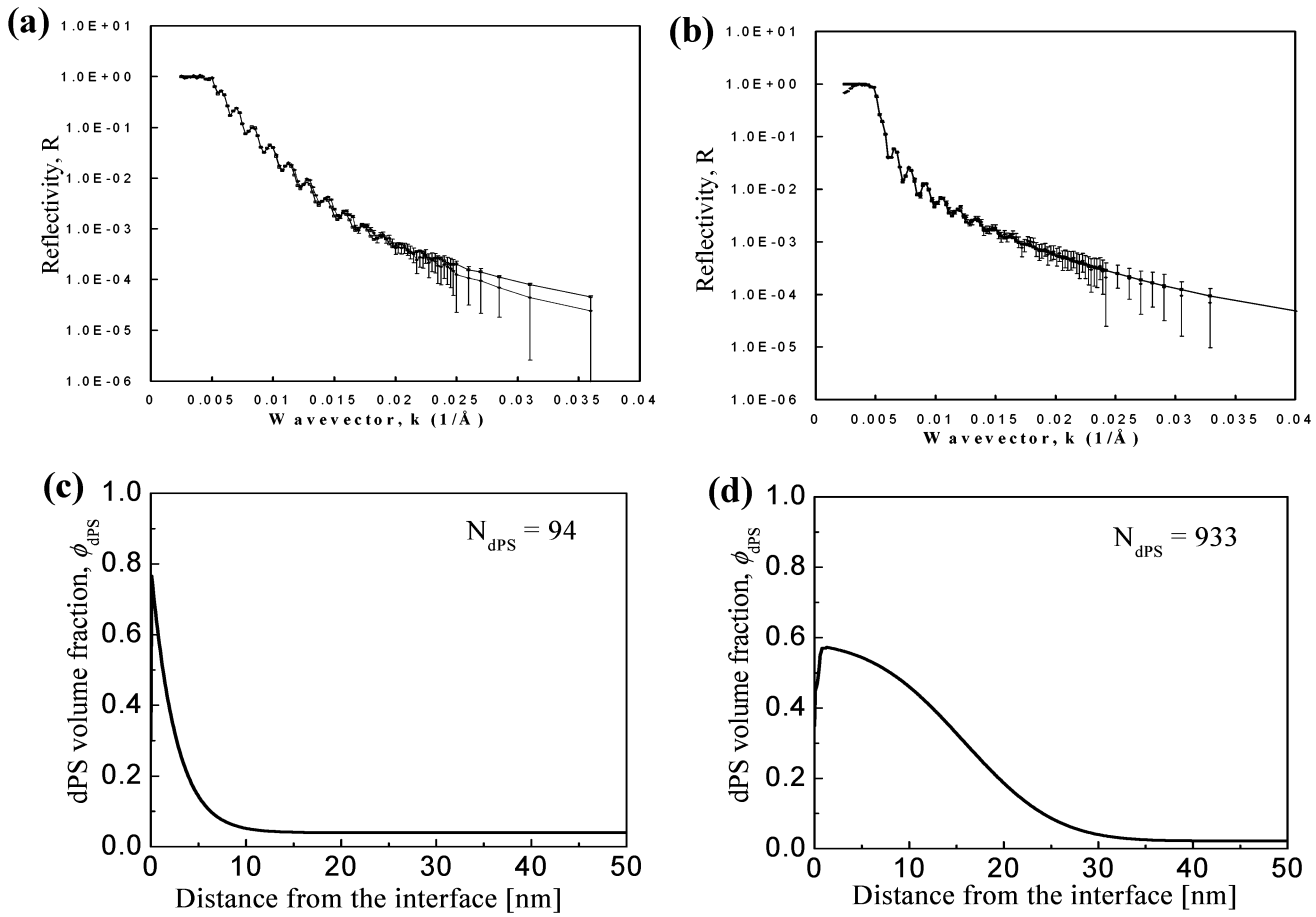

Figure 2. Reflectivity, R, vs wave vector, k, for PS:dPS-*b*-PMMA with $N_{dPS} = 94$ (a) and $N_{dPS} = 933$ (b). The solid circles in (a) and (b) represent experimental R whereas the solid lines are the calculated R using dPS volume fraction profiles, ϕ_{dPS}, (c) and (d), respectively. Details are given in the text. The z^*, w, and h values for these profiles are given in Figures 3, 6, and 7.

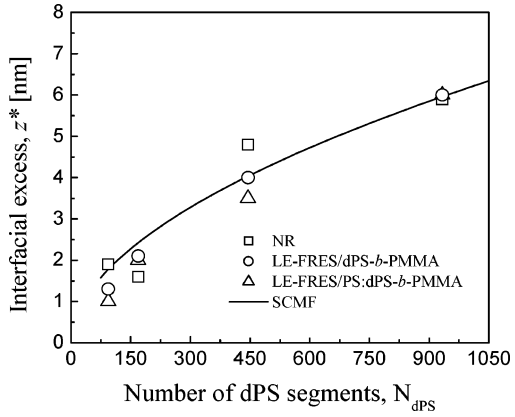

Figure 3. Interfacial excess, z^*, as a function of N_{dPS} for PS:dPS-*b*-PMMA as determined from LE-FRES (open triangles), NR (open squares), and SCMF model (solid line). The SCMF parameters are given in the text. LE-FRES was also done from physisorbed dPS-*b*-PMMA (open circles).

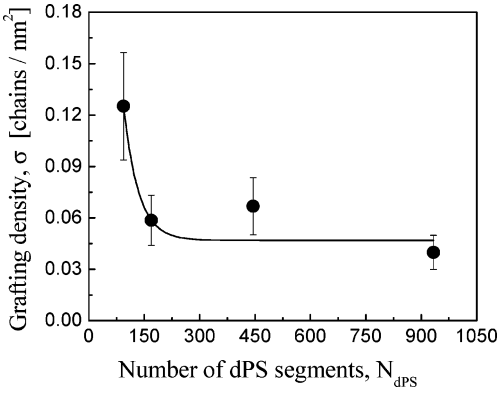

Figure 4. Grafting density, σ, as a function of N_{dPS} for PS:dPS-*b*-PMMA. The σ values (solid circles) were calculated using eq 2 and z^* values from NR. The solid line is a guide to the eye. The error bars represent ±10% of σ values and are in good agreement with the z^* variation in Figure 3.

that z^* values as low as 1 nm can be determined from films containing adsorbed copolymer. The z^* values measured by LE-FRES and NR are in good agreement, particularly at $N_{dPS} = 933$. The solid line is from values obtained by the SCMF calculations, which are discussed later.

Figure 4 shows σ as a function of N_{dPS} for the PS:dPS-*b*-PMMA system. The σ values were calculated using eq 2 and the z^* values obtained from NR. The σ initially decreases by a factor of 2.5 as N_{dPS} increases from 94 to 169 and then stays relatively constant as N_{dPS} increases further. Thus, as N_{dPS} increases and crowding increases, chains will stretch until the free energy gain obtained by reducing excluded-volume interactions is offset by the entropic penalty for stretching chains beyond their random walk conformation. Thus, a "brushlike" conformation is expected for copolymers having high values of N_{dPS} as observed in Figure 2d for $N_{dPS} = 933$. The z^* and σ values obtained in this paper are in good agreement with published values for equilibrium brushes in a melt[2,8−10] and solution.[25−27]

To investigate how chain stretching increases with N_{dPS}, the average distance between chains, D, has been

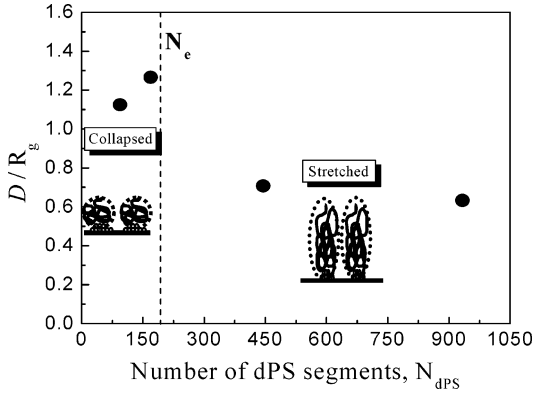

Figure 5. Distance between grafted chains normalized by R_g of the dPS block, D/R_g, as a function of N_{dPS} for PS:dPS-*b*-PMMA. The D values (solid circles) were calculated using eq 4 and σ values in Figure 4. The vertical dashed line represents the DP between entanglements of PS, N_e. A transition from collapsed ($D/R_g > 1$) to stretched ($D/R_g < 1$) chains (cf. inset adsorbed chains) occurs near $N_{dPS} \approx N_e$.

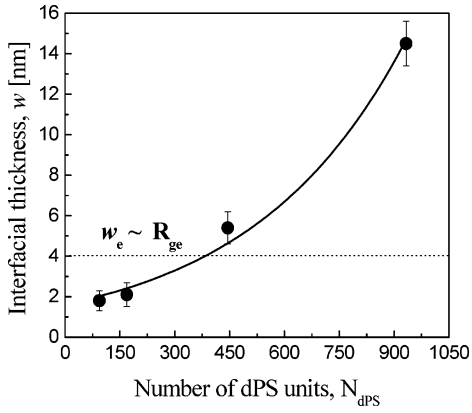

Figure 6. Interfacial width, w, as a function of N_{dPS} for PS:dPS-*b*-PMMA. The dashed line represents the interfacial width between entanglements of PS, w_e, which is given by $w_e = a(N_e/6)^{1/2}$, where a is the PS segment length. The solid line is a guide to the eye. The error bars represent ±10% of w values.

calculated:

$$D = \sigma^{-1/2} \tag{4}$$

For chains that are far apart relative to the radius of gyration of the dPS block, R_g, adsorbed copolymers exhibit a "mushroomlike" conformation.[28] For $D \approx R_g$, adsorbed copolymers can form clusters, whereas for $D < R_g$ a homogeneous monolayer is expected. Using eq 4 to calculate D, Figure 5 shows that D/R_g displays two regimes of behavior. For $N_{dPS} < 200$ ($\approx N_e$), D is greater than R_g and isolated chains adopt a "mushroomlike" conformation. For $N_{dPS} > 200$, D is less than R_g and chains stretch to form a "brushlike" conformation. Thus, the behavior of D/R_g is consistent with the dPS volume fraction profiles and σ results shown in Figures 2c,d and 4, respectively.

Figure 6 shows that the interfacial width, w, increases from 2 to ca. 15 nm as N_{dPS} increases from 94 to 933, respectively. The solid line is a guide to the eye. As a reference, the distance between entanglements in PS is plotted as a dotted line, $w_e \approx 4$ nm. Note that only the two highest molar mass copolymers exhibit an interfacial width that is broader than w_e. In particular, the interface between dPS-*b*-PMMA with $N_{dPS} = 933$ and the bulk is almost 3 times broader than w_e. Although all four dPS-*b*-PMMA copolymers show an interfacial excess, PS:dPS-*b*-PMMA films were able to prevent dewetting only when copolymers had $N_{dPS} > 200$.[19,29] These results suggest that copolymer segregation alone is not sufficient to prevent dewetting. But rather w values greater than w_e are required to strengthen the interface, reduce interfacial tension,[19,30] and thus decrease the dewetting driving force.[29] For immiscible polymer bilayers, Creton et al.[31] provided a similar argument about the role of N_e on the fracture toughness.

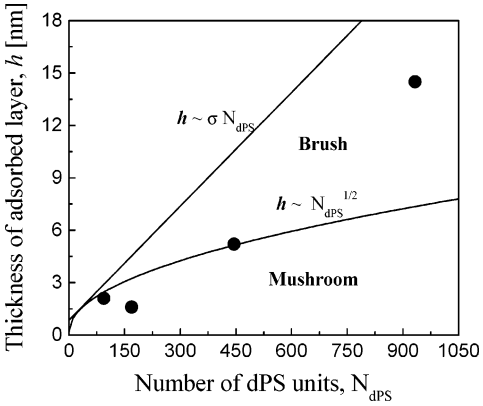

Figure 7. Thickness of adsorbed layer, h, as a function of N_{dPS} for PS:dPS-*b*-PMMA. The h values (solid circles) were calculated using eq 3 and z^* values from NR. The solid lines represent the scaling[32] of h for two regimes: mushroom where $h \sim N_{dPS}^{1/2}$, for $P > N_{dPS}^{1/2}$ (P is the matrix DP), and brush where $h \sim \sigma N_{dPS}$, for $P > N_{dPS}$.

Figure 7 shows that the thickness of the adsorbed layer, h, increases by a factor of 7 as N_{dPS} increases from 94 to 933. This increase in h is most notable as N_{dPS} increases from 455 to 933. Using σ, D/R_g, and $\phi(z)$ as guides, the scaling relationships[32] for mushroom and brush conformations have been plotted as solid lines in Figure 7. Comparison of the data with the scaling behavior suggests that the lowest N_{dPS} copolymers are unstretched and display h values consistent with a "mushroomlike" conformation, whereas the highest N_{dPS} copolymers are stretched with h values indicative of a "brushlike" conformation. Because of the limited data in each regime and small variations in N_{PMMA}, the comparison between the scaling predictions and the experimental data should be considered as qualitative only.

4.2. Interfacial Characteristics of PS:dPS-*b*-PDMAEMA Films. To understand the role of the anchor−substrate interaction, adsorption of dPS-*b*-PDMAEMA copolymers was investigated in PS:dPS-*b*-PDMAEMA films. The PS matrix had a $P = 1923$ ($>2N_{dPS}$), and 5 vol % of dPS-*b*-PDMAEMA was added. The interfacial characteristics for the two dPS-*b*-PDMAEMA copolymers are summarized in Table 3. Note that $N_{dPS} > N_e$ for both copolymers. The z^* values increase from 4.0 to 6.3 nm as N_{dPS} increases from 356 to 676, respectively. Moreover, z^* values from LE-FRES and NR are in good agreement. For both copolymers D/R_g is <1, consistent with a stretched chain conformation. In comparison with the PS:dPS-*b*-PMMA system (cf. Figure 3), the z^* values for the PS:dPS-*b*-PDMAEMA films are larger at similar N_{dPS}. As discussed below, the stronger adsorption of dPS-*b*-PDMAEMA is attributed to a greater attraction between the DMAEMA segments and SiO_x.

Similar to the behavior of z^*, h and w for PS:dPS-*b*-PDMAEMA films increase with increasing N_{dPS} as shown in Table 3. Using eq 3 and the profile from NR,

Table 3. Measured Interfacial Characteristics of PS:dPS-*b*-PDMAEMA Films

N_{dPS}	$N_{PDMAEMA}$	z^{*a} (nm)	z^{*b} (nm)	σ^b [chains/nm^2]	$D/R_g{}^b$	h^b (nm)	w^b (nm)
356	19	3.7	4.0	0.070	0.71	4.8	12.0
676	6	5.6	6.3	0.056	0.61	6.6	15.0

[a] z^* measured from LE-FRES. [b] z^*, w, h, determined from NR profiles. [c] σ and D calculated from z^* determined from NR.

h was calculated and found to increase from 4.8 to 6.6 nm as N_{dPS} increase from 356 to 676. Using the definition of w in Figure 1, w values increase from 12 to 15 nm as N_{dPS} increases. Thus, for both dPS-*b*-PDMAEMA copolymers, w is greater than the entanglement distance $w_e \approx 4$ nm. This broad interface between the dPS dangling block and the matrix chains suggests a reduction in interfacial tension[19,30] and a corresponding increase in film stability.[29] Experiments show that the addition of only 1 vol % dPS-*b*-PDMAEMA to a PS film (75 nm thick) prevents dewetting from SiO_x.

4.3. SCMF Simulations of Volume Fraction Profiles. The SCMF method requires knowledge of χ to calculate the volume fraction profile at the polymer/substrate interface. Thus, before investigating Σ, the χ parameters used in the SCMF calculations will be described. For the PS:dPS-*b*-PMMA system, the χ values are $\chi_{PMMA-dPS} = 0.0371$,[2,33,34] $\chi_{PMMA-hPS} = 0.0282$,[33,34] and $\chi_{hPS-dPS} \sim 0.0001$.[9] For the case of PS:dPS-*b*-PDMAEMA, the χ between PDMAEMA and the dPS block, $\chi_{PDMAEMA-dPS}$, as well as PDMAEMA and PS, $\chi_{PDMAEMA-PS}$, are unknown. Because a DMAEMA segment is more polar than MMA, the χ values for $\chi_{PDMAEMA-dPS}$ and $\chi_{PDMAEMA-PS}$ are expected to be greater than $\chi_{PMMA-dPS}$ and $\chi_{PMMA-PS}$, respectively. To understand the impact of $\chi_{PDMAEMA-dPS}$ and $\chi_{PDMAEMA-PS}$ on copolymer adsorption, SCMF simulations for PS:dPS-*b*-PDMAEMA with $N_{dPS} = 356$ were performed for two different cases, first assuming $\chi_{PDMAEMA-dPS} \approx \chi_{PMMA-dPS}$ and $\chi_{PDMAEMA-PS} \approx \chi_{PMMA-PS}$ and second assuming $\chi_{PDMAEMA-dPS} \approx 2\chi_{PMMA-dPS}$ and $\chi_{PDMAEMA-PS} \approx 2\chi_{PMMA-PS}$. However, for both sets of χ's, the model $\phi(z)$ profiles were in poor agreement with the experimental $\phi(z)$ profiles. The best agreement between the model and the experimental profiles occurs for χ values between these two cases, namely $\chi_{PDMAEMA-PS} = 0.055$ and $\chi_{PDMAEMA-dPS} = 0.042$. (cf. Figure 9b).

Knowing the χ parameters, SCMF calculations could be performed using a single fitting parameter that represents the attraction between the PMMA (or PDMAEMA) anchoring block and the SiO_x surface, namely $\Sigma_{PMMA-SiO_x}$ (or $\Sigma_{PMMAEMA-SiO_x}$). Parts a and b of Figure 8 show the $\phi(z)$ obtained from NR measurements for PS:dPS-*b*-PMMA films with $N_{dPS} = 94$ and $N_{PMMA} = 10$ (open circles) and $N_{dPS} = 445$ and $N_{PMMA} \approx 40$ (open squares), respectively. Using $\Sigma_{PMMA-SiO_x} = -7k_BT$ and $-11\ k_BT$, respectively, the profiles predicted by the SCMF model (solid lines) are in excellent agreement with the experimental profiles. The thin dPS depletion layer at the interface is due to adsorbed MMA segments. Including a depletion layer in the experimental profile does not improve the fitting in the NR simulation and is therefore left out for simplicity. Both profiles are exponential-like, in contrast to the parabolic profile observed in Figure 2d for the longest dPS block length. The agreement between the SCMF and the experimental dPS volume fraction profiles for dPS-*b*-PMMA with $N_{dPS} = 169$ and 933 are very good if a $\Sigma_{PMMA-SiO_x}$ value of $-11k_BT$ is used, consistent with the $N_{dPS} = 445$ case.

The interfacial characteristics obtained from the SCMF calculations for each dPS-*b*-PDMAEMA are given in Table 4. Note that the experimental z^*, σ, D, h, and w values (cf. Table 3) are in excellent agreement with those obtained by the SCMF model (cf. Table 4). The reflectivity from a PS:dPS-*b*-PDMAEMA film with $N_{dPS} = 676$ is shown in Figure 9a. The predicted reflectivity (solid line) was calculated assuming the exponential-like profile (open triangles) in Figure 9b. Using $\Sigma_{PDMAEMA-SiO_x} = -7k_BT$, the SCMF profile (solid line) is in very good agreement with the experimental profile. The dPS volume fraction profile for PS:dPS-*b*-PDMAEMA film with $N_{dPS} = 356$ has been omitted due to space limitations. This profile shape is also exponential-like and in excellent agreement with the SCMF profile using $\Sigma_{PDMAEMA-SiO_x} = -14k_BT$.

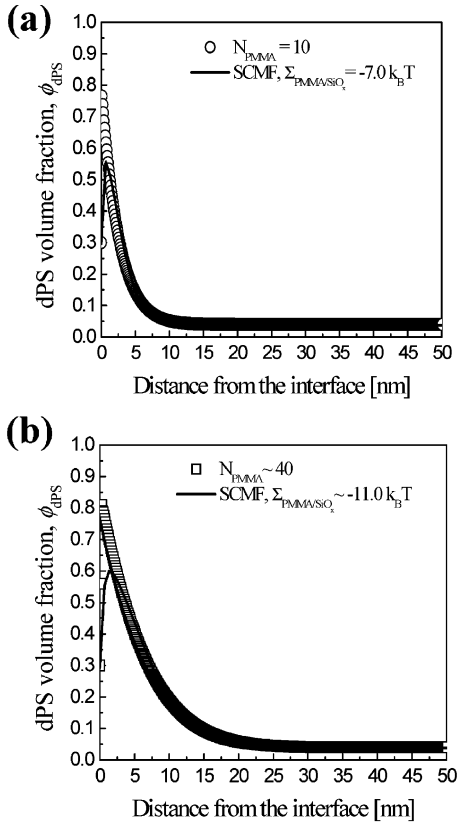

Figure 8. Volume fraction profiles of dPS block, ϕ_{dPS}, determined from NR for PS:dPS-*b*-PMMA with (a) $N_{PMMA} = 10$ (open circles) and (b) $N_{PMMA} \approx 40$ (open squares). The dPS/SiO_x interface is located at depth 0. The solid lines represent the ϕ_{dPS} profiles calculated by SCMF for $\Sigma_{PMMA-SiO_x}$ values of $-7k_BT$ (a) and $-11k_BT$ (b).

Table 4. SCMF Values of Interfacial Characteristics of PS:dPS-*b*-PDMAEMA Films

N_{dPS}	$N_{PDMAEMA}$	z^* (nm)	σ [chains/nm^2]	D/R_g	h (nm)	w (nm)
356	19	3.6	0.062	0.77	5.0	14.0
676	6	5.7	0.052	0.63	6.6	16.0

4.4. Determination of Interaction Energies per Segment. The interaction energies between each adsorbing segment and the substrate, ϵ, are not readily available. In this section, the ϵ values for MMA (DMAEMA) and SiO_x as well as the dependence of Σ on N_{PMMA}

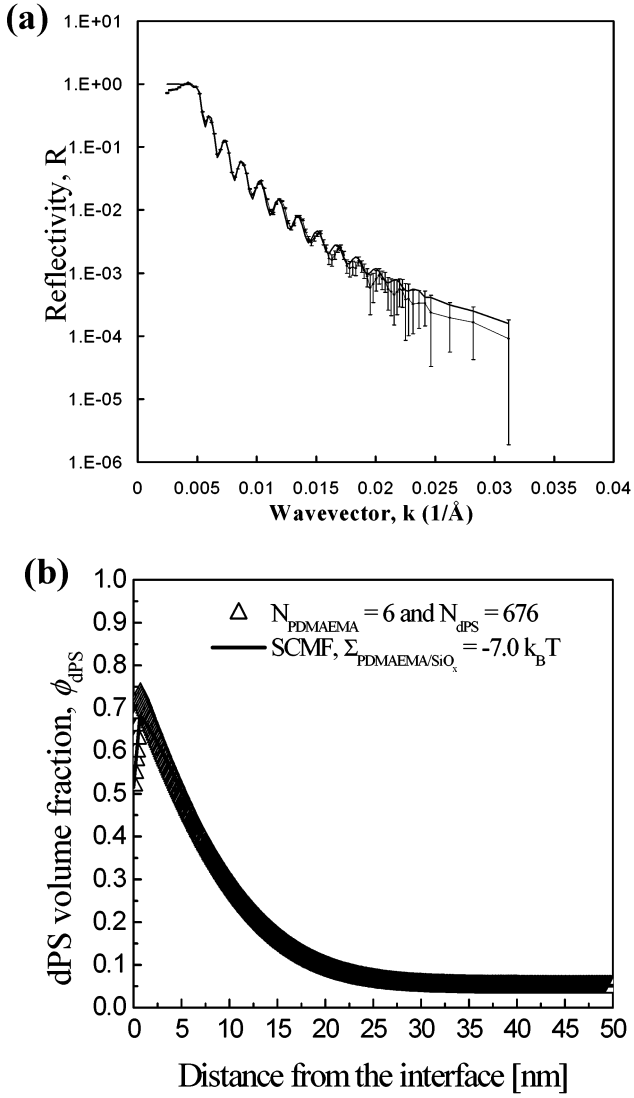

Figure 9. Reflectivity, R, vs wave vector, k, for PS:dPS-*b*-PDMAEMA with $N_{dPS} = 676$ (a). In (a) the solid circles represent experimental R whereas the solid line is the calculated R using the dPS volume fraction profile, ϕ_{dPS}, (b) determined from NR (open triangles). The dPS/SiO_x interface is at depth 0. In (b) the solid line represents the ϕ_{dPS} profile calculated by SCMF using $\Sigma_{PDMAEMA-SiO_x} = -7k_BT$.

($N_{PDMAEMA}$) are investigated. In the SCMF simulations described above Σ varies from $-7k_BT$ to $-11k_BT$ for $N_{PMMA} = 10$ and ≈ 40, respectively, and from $-7k_BT$ to $-14k_BT$ for $N_{PDMAEMA} = 6$ and 19, respectively. The negative sign indicates segmental attraction to SiO_x. This dependence of Σ on N has been reported by others[35] but never fully explained.

The molar mass dependence of Σ can be understood by considering the fraction of anchoring block segments in direct contact with the substrate, f. Thus, Σ is given by $f\epsilon N$. For $f = 1.0$, at 100% adsorption, ϵ would be simply given by Σ/N. If the anchor block contains many loops and tails, f is small and so is Σ. A key test is whether a single value of ϵ can describe each set of data. Although f is difficult to measure, physically reasonable values of f can be estimated from N and σ.

For the PS:dPS-*b*-PMMA system, the PMMA block length was either long ($N_{PMMA} \approx 40$) or short ($N_{PMMA} = 10$) (cf. Table 1). For the long PMMA block nearly a third of the monomers are assumed to be in direct contact with the substrate (i.e., trains) and $f \approx 0.35$. From Figure 4, the shorter PMMA block (with $N_{dPS} = 94$) has a σ that is about 2.5 times greater than the long PMMA block case. So, we estimate that $f \approx 0.90$ ($= 0.35 \times 2.5$). This value is consistent with shorter chains tending to form trains whereas long ones tend to have more loops and tails. Using $f = 0.35$ and 0.90 for long and short PMMA blocks, respectively, a constant value for ϵ can be extracted, namely, $-0.8 \pm 0.1k_BT$.

For PS:dPS-*b*-PDMAEMA films, comparison between the experimental and the SCMF volume fraction profiles yield Σ values of $-14k_BT$ and $-7k_BT$ for $N_{dPS} = 356$ and 676, respectively. The grafting densities for these copolymers are similar, $\approx$0.070 and 0.056 chains/nm^2, respectively (cf. Table 3). Because the anchoring blocks for both copolymers are very short ($N_{PDMAEMA} = 19$ and 6), both PDMAEMA blocks are taken to have a high fraction of segments in direct contact with the substrate. Using σ and $N_{PDMAEMA}$ as a guide, $f \approx 0.75$ and 1 for $N_{PDMAEMA} = 19$ and 6, respectively, yields a constant ϵ of $-1.1 \pm 0.1k_BT$.

By making physically reasonable assumptions about f, the SCMF provides a powerful method to extract the segmental attraction of MMA and DMAEMA for silicon oxide. Although both values of ϵ are about k_BT, the DMAEMA segment shows a slightly stronger attraction for the oxide than MMA. This attraction may be due to the amino group on DMAEMA that is lacking on MMA. Thus, the DMAEMA segments may interact more strongly with the Si−OH groups via hydrogen bonding and induced dipole−dipole interactions. This observation is consistent with the greater z^* values observed for PS:dPS-*b*-PDMAEMA relative to PS:dPS-*b*-PMMA.

5. Conclusions

In this paper, adsorption of dPS-*b*-PMMA and dPS-*b*-PDMAEMA from a PS neutral matrix to the melt/SiO_x interface is studied using LE-FRES and NR. For the dPS-*b*-PMMA system, the nonadsorbing block length, N_{dPS}, is varied from below N_e to above N_e, where N_e of PS is $\sim$200. For $N_{dPS} < 200$, the distance between grafted copolymer chains, D, is greater than the dPS radius of gyration, R_g, whereas for $N_{dPS} > 200$, D is less than R_g. Thus, a crossover from a collapsed to a stretched conformation occurs near $N_{dPS} \approx N_e$. Correspondingly z^*, w, and h strongly increase as N_{dPS} increases. Using the adsorbing block−substrate interaction, Σ, which varies with adsorbing block length, as a fitting parameter, SCMF predictions of $\phi(z)$, z^*, w, and h are in very good agreement with experimental results. This adsorbing block length dependence of Σ is explained by considering the fraction of MMA and DMAEMA segments in direct contact with the wall. Thus, segmental interaction energies between each MMA and DMAEMA segment with SiO_x are determined and about $-0.8k_BT$ and $-1.1k_BT$, respectively. This slight increase is consistent with the higher polarity of the PDMAEMA block in comparison to PMMA. We hope that this fundamental study of block copolymer adsorption contributes to the understanding needed to improve control over adhesion in polymeric coatings.[36]

Acknowledgment. We gratefully acknowledge support from ACS/PRF 38027/34081, NSF/Polymers (DMR02-34903 and INT99-75486), and NSF/MRSEC (DMR00-79909) for personnel and facility support as well as a collaboration grant from the U.S.−Czech Republic Science and Technology Program, Grant 203/

01/0513. Dr. Sushil Satija and Dr. Robert Ivkov (NIST) are acknowledged for their assistance with carrying out the reflectivity experiments.

References and Notes

(1) Zhao, X.; Zhao, W.; Zheng, X.; Rafailovich, M. H.; Sokolov, J.; Schwarz, S. A.; Pudensi, M. A. A.; Russell, T. P.; Kumar, S. K.; Fetters, L. J. *Phys. Rev. Lett.* **1992**, *69*, 776−779.
(2) Oslanec, R.; Vlček, P.; Hamilton, W. A.; Composto, R. J. *Phys. Rev. E* **1997**, *56*, 2383−2386.
(3) Liu, Y.; Schwarz, S. A.; Zhao, W.; Quinn, J.; Sokolov, J.; Rafailovich, M.; Iyengar, D.; Kramer, E. J.; Dozier, W.; Fetters, L. J.; Dickman, R. *Europhys. Lett.* **1995**, *32*, 211−216.
(4) Green, P. F.; Russell, T. P. *Macromolecules* **1992**, *25*, 783−787.
(5) Clarke, C. J.; Jones, R. A. L.; Edwards, J. L.; Clough, A. S.; Penfold, J. *Polymer* **1994**, *35*, 4065−4071.
(6) Jones, R. A. L.; Norton, L. J.; Shull, K. R.; Kramer, E. J.; Felcher, G. P.; Karim, A.; Fetters, L. J. *Macromolecules* **1992**, *25*, 2359−2368.
(7) Budkowski, A.; Klein, J.; Fetters, L. J. *Macromolecules* **1995**, *28*, 8571−8578.
(8) Oslanec, R.; Brown, H. R. *Macromolecules* **2001**, *34*, 9074−9079.
(9) Oslanec, R.; Composto, R. J.; Vlček, P. *Macromolecules* **2000**, *33*, 2200−2205.
(10) Retsos, H.; Terzis, A. F.; Anastasiadis, S. H.; Anastassopoulos, D. L.; Toprakcioglu, C.; Theodorou, D. N.; Smith, G. S.; Menelle, A.; Gill, R. E.; Hadziioannou, G.; Gallot, Y. *Macromolecules* **2002**, *35*, 1116−1132.
(11) Wang, J. S.; Binder, K. *J. Phys. I* **1991**, *11*, 1583−1590.
(12) Szleifer, I. *Europhys. Lett.* **1998**, *44*, 721−727.
(13) Ou-Yang, H. D.; Zihao, G. *J. Phys. II* **1991**, *1*, 1375−1385.
(14) Binder, K.; Müller, M.; Schmid, F.; Wener, A. *Physica A* **1998**, *249*, 293−300.
(15) Kim, S. H.; Jo, W. H. *J. Chem. Phys.* **1999**, *110*, 12193−12201.
(16) Genzer, J.; Composto, R. J. *Macromolecules* **1970**, *3*, 870−878.
(17) Brandrup, J.; Immergut, E. H.; Grulke, E. A. *Polymer Handbook*, 4th ed.; Wiley: New York, 1999.
(18) Dreux, P. C. Ph.D. Thesis, University of Pennsylvania, Philadelphia, PA, 1997.
(19) Costa, A. C.; Composto, R. J.; Vlček, P. *Macromolecules* **2003**, *36*, 3254−3260.
(20) Composto, R. J.; Walters, R. M.; Genzer, J. *Mater. Sci. Eng. Rep.* **2002**, *R38*, 107−180.
(21) Russell, T. P. *Mater. Sci. Rep.* **1990**, *5*, 171−271.
(22) Press, W. H.; Teukolsky, S. A.; Vetterling, W. T.; Flannery, B. P. *Numerical Recipes in C: The Art of Scientific Computing*, 2nd ed.; Cambridge University Press: Cambridge, UK, 1992.
(23) Shull, K. R.; Kramer, E. J. *Macromolecules* **1990**, *23*, 4769−4779.
(24) Shull, K. R. *J. Chem. Phys.* **1991**, *94*, 5723−5738.
(25) Dorgan, J. R.; Stamm, M.; Toprakcioglu, C. Jerome, R.; Fetters, L. J. *Macromolecules* **1993**, *26*, 5321−5330.
(26) Field, J. B.; Toprakcioglu, C.; Ball, R. C.; Stanley, H. B.; Dai, L.; Barford, W.; Penfold, J.; Smith, G.; Hamilton, W. *Macromolecules* **1992**, *25*, 434−439.
(27) Field, J. B.; Toprakcioglu, C.; Dai, L.; Hadziioannou, G.; Smith, G.; Hamilton, W. J. *J. Phys. II* **1992**, *2*, 2221−2235.
(28) Jones, R. A. L.; Richards, R. W. *Polymers at Surfaces and Interfaces*; Cambridge University Press: Cambridge, UK, 1999.
(29) Oslanec, R.; Costa, A. C.; Composto, R. J.; Vlček, P. *Macromolecules* **2000**, *33*, 5505−5512.
(30) Akpalu, Y. A.; Karim, A.; Satija, S. K.; Balsara, N. P. *Macromolecules* **2001**, *34*, 1720−1729.
(31) Creton, C.; Kramer, E. J.; Hadziioannou, G. *Macromolecules* **1991**, *8*, 1846−1853.
(32) de Gennes, P. G. *Macromolecules* **1980**, *13*, 1069−1075.
(33) Russell, T. P.; Hjelm, R. P., Jr.; Seeger, P. A. *Macromolecules* **1990**, *23*, 890−893.
(34) Russell, T. P. *Macromolecules* **1993**, *26*, 5819.
(35) Calistri,Y. M. Ph.D. Thesis, Cornell University, Ithaca, NY, 1995.
(36) Schnell, R.; Stamm, M.; Creton, C. *Macromolecules* **1998**, *31*, 2284−2292.

MA0348324